https://doi.org/10.48048/tis.2022.4605

# Theoretical Analysis of Adaptive Algorithm Modulation Scheme in 3D OFDM WiMAX System

**Valentin Petrovich Fedosov, Jaleel Sadoon Jameel* and Svetlana Valentinovna Kucheryavenko**

*Institute for Radiotechnical Systems and Control, Southern Federal University, Rostov-on-Don, Russia*

**(*Corresponding author's e-mail: Jaleel.s.jameel@mail.ru)**

*Received: 17 March 2021, Revised: 8 June 2021, Accepted: 8 July 2021*

**Abstract**

The growth of wireless networking has contributed to the need for high-speed services and multimedia applications anywhere and at any time. OFDM WiMAX technology is now considered one of the most popular technologies capable of delivering faster implementation and lower cost than standard wired options for Broadband Wireless Connectivity in metropolitan areas. This paper proposes appropriate adaptive modulation to be used in wireless networks based on SISO and MIMO OFDM WiMAX, which allows the performance of the network to be improved in the case of non-line-of-sight communications that are typical in urban environments. The effects of several paths, signal attenuation, Doppler shift, and different mobility speeds on the performance of the system were investigated. Mathematical models analysis of adaptive modulation in SISO and MIMO systems is treated by using BER, SNR and noise components. Simulation results show that the adaptive algorithm would improve throughput. It can also be concluded that when processing signals in a receiving system under conditions of multi-path signal propagation, the use of adaptive algorithms has a positive effect on noise immunity.

**Keywords***:* 3GPP 3D channel model, MIMO, SISO, OFDM wireless, Elevation angles, Doppler shift

## Introduction

Today, high data rate services, multimedia applications, and high-quality streams of information are in high demand and will continue in the near future. Wireless systems, for mobile users, are considered a viable and attractive solution for providing high data rates [1].

The Physical and Medium Access Control (MAC) layer specifications for a Broadband Wireless Access (BWA) communication protocol have recently been provided by the IEEE 802.16 family of standards [2,3] and sponsored by the WiMAX commercial consortium. The use of Orthogonal Frequency Division Multiplexing (OFDM) to mitigate the adverse effects of frequency-selective multi-path fading and efficiently contrast inter-symbol and inter-carrier interferences (ISI and ICI) is among several alternatives to the IEEE 802.16 standards [4]. In particular, our focus is on the multiple orthogonal frequency division scheme, which forms the basis of the WiMAX system [1,3].

OFDM is a digital modulation technique in which a signal at different frequencies is split up into several constricted band channels [5]. The main advantage of OFDM over single-carrier techniques is its ability to cope without complex equalization filters with harsh channel conditions since OFDM uses many slowly modulated constricted band signals rather than 1 rapidly modulated broadband signal [6]. To reduce multipath fading and inter carrier/symbol interference [7], the multi-carrier modulation characteristic of OFDM is useful in modern wireless technologies.

In wireless communications, adaptive modulation is used to refer to the similarity in modulation, coding and other signal and protocol parameters to the radio link stipulations [8]. There are different coding schemes involved in OFDM, such as QPSK, BPSK, 8PSK, and QAM16. Depending on the values of a certain parameter such as: Bit Error Rate (BER) and Signal to Noise Ratio (SNR), the choice of a particular scheme is considered [9]. Such parameters affect the channel efficiency. The limits of channel estimation decide the coding scheme that should be used for this particular signal received [10]. Due to its advanced 2D pilot-based channel estimation scheme in the time and frequency domain, WiMAX is more robust for high Doppler fast fading mobile channels [11].

A 3D channel model that accurately accounts for the elevation angles of the rays is carried out to accurately determine the efficiency of the Multiple Input Multiple Output (MIMO) and single-input single-output (SISO) techniques in WiMAX. The 3D WiMAX channel model implemented has been verified and a good match with ray tracer statistics is maintained [12,13]. The concept of 2D propagation breaks down as the distribution of the elevation angle is significant in some environments. In such situations, channel capacity estimation and system-level performance can lead to imprecise results. When modeling the communication channel, measured 3D radiation patterns are used for macro-cell Base Station (BS) and user equipment (UE) antennas [12]. Employing adaptive modulation scheme in wireless propagation environments over fading networks would result in great performance enhancements.

**Adaptive signal processing algorithm**

In the general case, the receiving antenna array is separated into different blocks; in the case of the SISO system, there is a single antenna array (AR); and in the case of the MIMO system, AR is further divided into blocks forming the receiving antennas [14,15]. The methodology considered is based on the use of phase AR [16]. This algorithm is based on the calculation of the correlation matrix's eigenvalues and eigenvectors. The block diagram of the adaptive unit in the receiver for the MIMO system is shown in **Figure 1**. The SISO system adaptive block is similar, except that there will be 1 adaptation block and no space-time decoder is available. The receiving antenna array in an adaptive processing system is an AR consisting of N elements that form adaptive processing units. The process of forming adaptive directional characteristic provides not only the formation of a maximum in the direction of the path with the greatest power, but also the formation of zeros in the direction of the remaining paths. In this regard, there are restrictions on the choice of the number of AR elements, depending on the number of independent flows that must be obtained after adaptation, and the number of AR elements in a block depends on the number of paths. In addition, the width of the resulting directivity characteristics depends on the number of elements in the block.

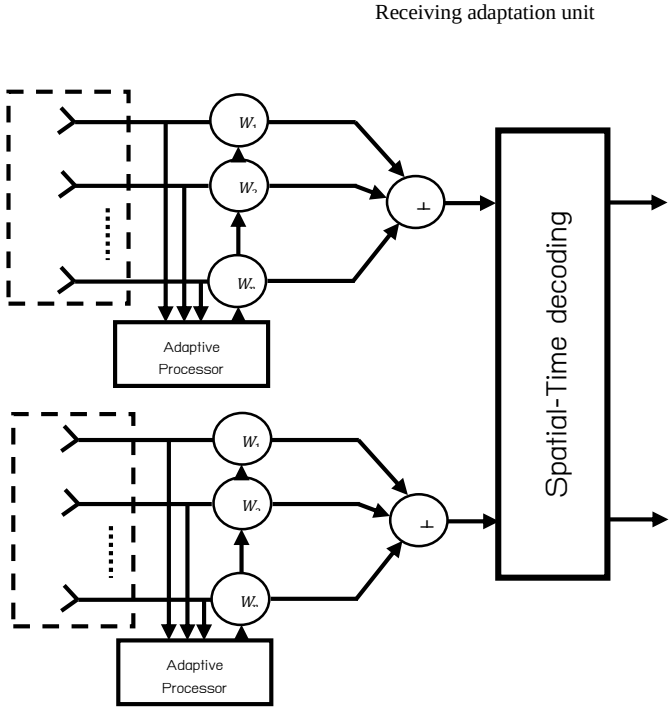


**Figure 1** Adaptive processing block diagram.

As shown in **Figure 1**, the signal at the output of each adaptation block can be expressed as:

$$Y(t) = \sum_{i=1}^{N} w_i x_i(t) = W^H X(t) \quad (1)$$

where $w_i$ are the values of ith weight vector; $x_i$ - samples of ith input signal and $N$ is the number of AR elements in one block.
The received signal $X(t)$ can be written as the sum of the useful signal $S(t)$ and interference component $N(t)$ [17].

$$X(t) = S(t) + N(t) \tag{2}$$

As a result of weight processing, the output of the adaptive block will be an output signal that should contain a signal from the path with the highest power and a minimum from other directions. Thus, the task is to determine the optimal weight vector ($W_{opt)}$ that maximizes the SNR [17].

$$q = \frac{W^H R_{ss} W}{W^H R_{nn} W} \tag{3}$$

where $R_{ss}$ is the spatial correlation matrix of the signal; $R_{nn}$ is the spatial correlation matrix of noise, W is the weight vector and $(\,)^H$ is the complex conjugation transposition operation (or Hermitian transposition).
The correlation matrix is Hermitian and is defined as follows:

$$R_{ss}(i,j) = E\{X(i).X^H(j)\} = \frac{1}{L}\sum_{i=0}^{L-1} X(i).X^H(j) \tag{4}$$

where $X$ is the input signal vector; $L$ is the number of samples of the input signal.
For any Hermitian matrix, the relation that is known from linear algebra, which is known as spectral decomposition (a set of eigenvalues), is valid, therefore, formula expression (4) can be written as:

$$R_{YY} = V\Lambda V^H \tag{5}$$

where $V$ is the unitary matrix of eigenvectors; Λ is the diagonal matrix of eigenvalues $\lambda_n$

$$V = [V_1 \quad V_2 \cdots V_n], \Lambda = \begin{bmatrix} \lambda_1 & 0 & 0 \\ 0 & \ddots & 0 \\ 0 & 0 & \lambda_n \end{bmatrix} \tag{6}$$

Since the columns and rows of the matrix V are mutually orthogonal and normalized, then

$$VV^H = V^H V = I \tag{7}$$

where $I$ is the identity matrix. It follows that

$$V^{-1} = V^H \tag{8}$$

The criterion for minimizing the output power of interference and noise provides an eigenvector of the matrix R corresponding to its maximum eigenvalue.
After calculating the optimal vector, the input signal is weighted, as a result, the signal from the adaptive processing unit can be written as:

$$Y_W = Y^H W_{opt} \tag{9}$$

The signal at the output of the adaptation block can be written as

$$Y_W = H_W X + N \tag{10}$$

where $H_W$ is the modified channel matrix after weight processing

$$H_w = HW_{opt} \tag{11}$$

**System model**

If a straight line can be established between the network cells without any obstacles, a wireless communication connection between a transmitter (Tx) and a receiver (Rx) is known as a line of sight (LOS). Connection condition, i.e. if the path is LOS or non-line-of-sight (NLOS), specifies in channel models several important parameters, including the path loss (PL), angle distribution, etc. [18]. An adaptive algorithm 3D channel model based on antenna arrays that accounts for the elevation angles of the rays is carried out to accurately evaluate the performance of MIMO systems in WiMAX. The adaptive processing unit will only be in the receiver and non-directional transmission will be performed by the transmitter. Adaptive signal processing can be extended to both conventional one receiving and one transmitting antenna communication systems, and spatial signal processing communication systems using a combination of antenna array transmitting and receiving elements. It was selected the carrier frequency of 2.5 GHz for each pair of transmitting and receiving antennas, which will have moderate signal attenuation for the wireless range selected. The distance and height of the base and mobile station location will be selected from the intended operation of the communication system in the 100 m high and 25 km range zone.

Channel propagation models are shown in **Figures 2** and **3** below. **Figure 2** shows the propagation paths in the XZ plane between the mobile and base station, where reflections are shown from the buildings and objects, where the direct path is also shown. **Figure 3** shows a geometric model in the XY plane, which shows the reflections of signals from the buildings and the objects. The multi-path propagation of waves from buildings and objects is considered in this paper. A long-range communication system is considered by the model and is characterized by the presence of a direct LOS path or its absence of NLOS.

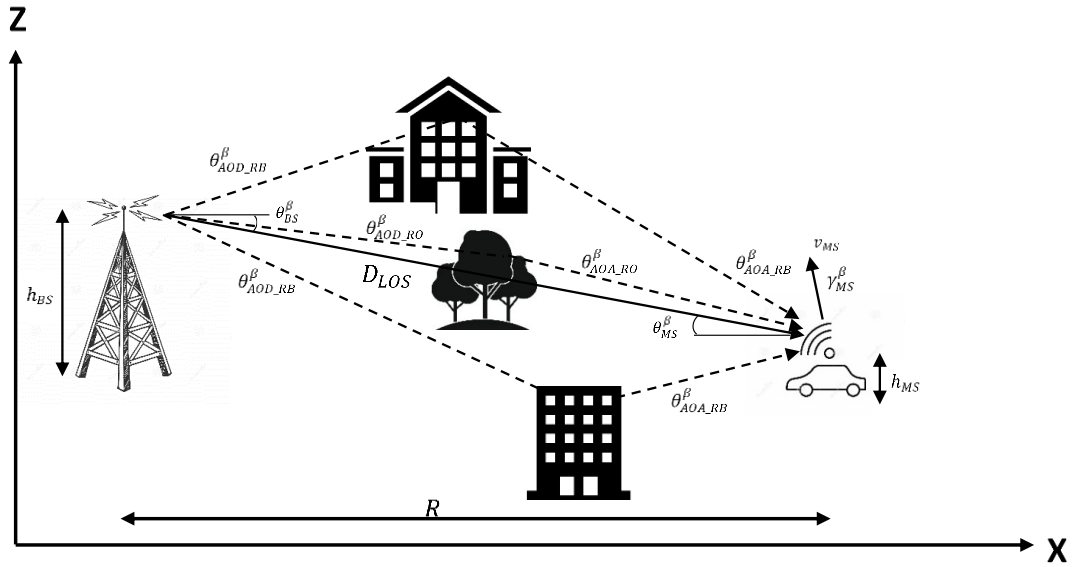


**Figure 2** Propagation model channel in the XZ plane.

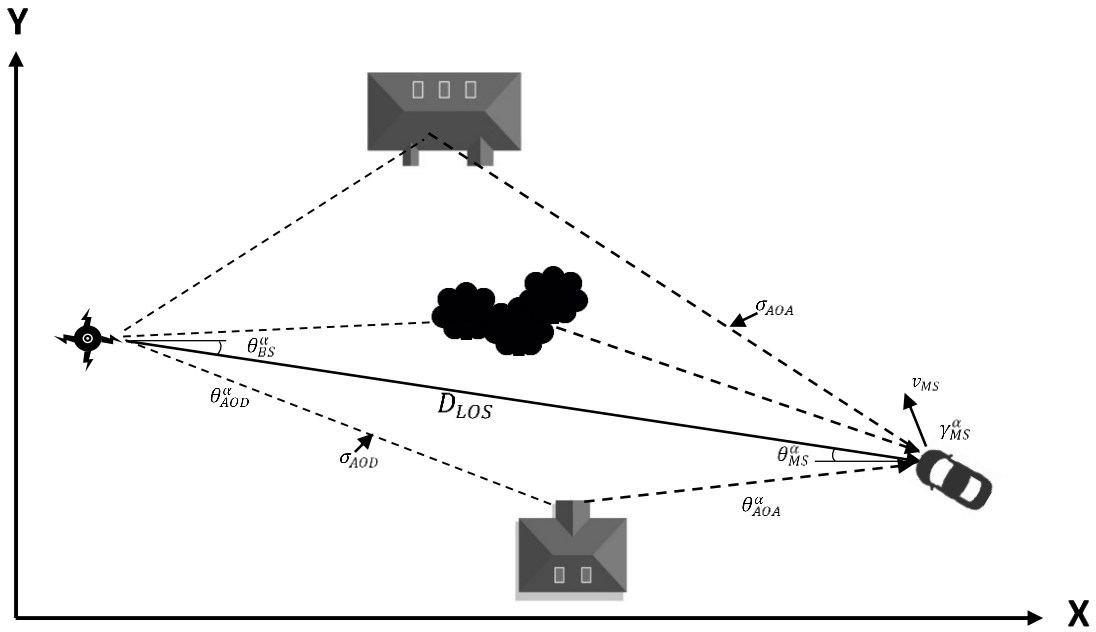


**Figure 3** Propagation model channel in the XY plane.

The locations of the BS transmitter and the MS receiver are defined by the high value $h_{BS}$, $h_{MS}$ and horizontal distance R. The horizontal distance takes into account the position of the base and mobile stations on the plane. In the figure, the straight path is characterized by the $D_{LOS}$ length and angles for the azimuth plane $\theta_{BS}^{\alpha}$ and $\theta_{MS}^{\alpha}$, and for the elevation plane $\theta_{BS}^{\beta}$ and $\theta_{MS}^{\beta}$ that are calculated by known distance and high. The receiver can move relative to transmitter, and this movement is described by the velocity vector $v_{MS}$, and the direction of the velocity vector is given by the angles $\gamma_{MS}^{\alpha}$ and $\gamma_{MS}^{\beta}$. The signal emission angles of a transmitting antenna $\theta_{AOD}^{\alpha}$, $\theta_{AOD}^{\beta}$, i.e., angles of departure (AoD), and $\theta_{AOA}^{\alpha}$, $\theta_{AOA}^{\beta}$, i.e. angles of arrival (AoA) at the reception, are characterized by a random value, which is set as an offset relative to the main path. The spread of subpaths, relative to the main path, is characterized by the values $\sigma_{AOD}$ and $\sigma_{AOA}$, for simplicity are considered the same in both planes.

As a result, the impulse response of a multi-path channel can be described by the following expression [19].

$$h(t,\tau) = \sum_{n=1}^{N} a_n(t)\delta(\tau - \tau_n(t)) \quad (12)$$

where $a_n(t)$ is the time-varying amplitude of the nth path, $\tau_n(t)$ is the time-varying propagation delay of the signal for the nth path, N is the number of paths.

For the 3D WiMAX channel under consideration, the impulse response will have the form.

$$h(t,\tau) = h^{LOS}(t,\tau) + h^{RB}(t,\tau) + h^{RO}(t,\tau) \quad (13)$$

where $h^{LOS}(t,\tau)$ is the component describing the direct path; $h^{RB}(t,\tau)$ the component describes reflection from the building; $h^{RO}(t,\tau)$ the component describes the reflection from the Objects.

Eq. (1) defines all the components of the signals that come from the direct direction and the directions of the reflections. Each component contains n reflected signals in addition to the direct path. The number of reflected signals depends on the distance and the number of buildings between the receiver and the transmitter. The situation becomes more complicated if the mobile station continues travelling relative to the base station. This leads to the addition of a doppler frequency shift to the multipath components.

The mathematical representation of the direct path $h_{s,u}^{LOS}(t,\tau)$ is written as [20,21].

$$h_{s,u}^{LOS}(t,\tau) = \sqrt{\frac{K}{K+1}}.\sqrt{G_{BS}\left(\theta_{BS}^{\alpha},\theta_{BS}^{\beta}\right)}.\sqrt{G_{MS}\left(\theta_{MS}^{\alpha},\theta_{MS}^{\beta}\right)}.L_S(D_{LOS}).L_A(D_{LOS}).$$
$$\delta(\tau-\tau_{LOS})\exp(jkd_{BS}^{1}\sin(\theta_{BS}^{\alpha}))\exp\left(jkd_{BS}^{2}\sin\left(\theta_{BS}^{\beta}\right)\right)$$
$$\exp(jkd_{MS}^{1}\sin(\theta_{MS}^{\alpha}))\exp\left(jkd_{MS}^{2}\sin\left(\theta_{MS}^{\beta}\right)\right)$$
$$\exp(jK[v_{BS}\cos(\theta_{BS}^{\alpha}-\gamma_{BS}^{\alpha})\cos\left(\theta_{BS}^{\beta}-\gamma_{BS}^{\beta}\right)+\ v_{MS}\cos(\theta_{MS}^{\alpha}-\gamma_{MS}^{\alpha})\cos\left(\theta_{MS}^{\beta}-\gamma_{MS}^{\beta}\right)]t) \quad (14)$$

where K is the Rice coefficient; s is the number of antenna elements of the base station; u is the number of antenna elements of the mobile station; $d_{BS}^{1}$ – the distance between the elements of the base station antennas in the horizontal plane; $d_{BS}^{2}$– the distance between the elements of the base station antennas in the vertical plane; $d_{MS}^{1}$– the distance between the mobile station elements of the mobile station in the horizontal plane; $d_{MS}^{2}$ – the distance between the mobile station elements of the mobile station in the vertical plane; $L_s(D)$ – loss upon propagation of the wave [22]; $G_{BS}\left(\theta^{\alpha},\theta^{\beta}\right)$– the gain of the transmitting antenna in the direction of the reflectors; $G_{MS}\left(\theta_{MS}^{\alpha},\theta_{MS}^{\beta}\right)$– is the gain of the receiving antenna of the mobile station.

Components describing reflection from buildings, $h_{s,u,n}^{RB}(t,\tau)$, and objects, $h_{s,u,n}^{RO}(t,\tau)$, can be represented, respectively, as [23,24].

$$h_{s,u,n}^{RB}(t,\tau) = \sqrt{\frac{1}{K+1}}.L_S(D_n).\frac{1}{\sqrt{M}}.\sum_{m=1}^{M}\frac{\sqrt{G_{BS}\left(\theta_{AOD_{RB},n,m}^{\alpha},\theta_{AOD_{RB},n,m}^{\beta}\right)}}{\sqrt{G_{MS}\left(\theta_{AOA\_RB,n,m}^{\alpha},\theta_{AOA\_RB,n,m}^{\beta}\right)}}$$
$$\xi_{n,m}\emptyset_{n,m}\exp\left(jkd_{BS}^{1}\sin\left(\theta_{AOD\_RB,n,m}^{\alpha}\right)\right)\exp\left(jkd_{BS}^{2}\sin\left(\theta_{AOD\_RB,n,m}^{\beta}\right)\right)$$
$$\exp\left(jkd_{MS}^{1}\sin\left(\theta_{AOA\_RB,n,m}^{\alpha}\right)\right)\exp\left(jkd_{MS}^{2}\sin\left(\theta_{AOA\_RB,n,m}^{\beta}\right)\right)$$
$$\exp(jK[v_{BS}\cos\left(\theta_{AOD\_RB,n,m}^{\alpha}-\gamma_{BS}^{\alpha}\right)\cos\left(\theta_{AOD\_RB,n,m}^{\beta}-\gamma_{BS}^{\beta}\right)+$$
$$v_{MS}\cos\left(\theta_{AOA\_RB,n,m}^{\alpha}-\gamma_{MS}^{\alpha}\right)\cos\left(\theta_{AOA\_RB,n,m}^{\beta}-\gamma_{MS}^{\beta}\right)]t) \quad (15)$$

$$h_{s,u,n}^{RG}(t,\tau) = \sqrt{\frac{1}{K+1}}.L_S(D_n).\frac{1}{\sqrt{M}}\sum_{m=1}^{M}\frac{\sqrt{G_{BS}\left(\theta_{AOD_{RG},n,m}^{\alpha},\theta_{AOD_{RG},n,m}^{\beta}\right)}}{\sqrt{G_{MS}\left(\theta_{AOA\_RB,n,m}^{\alpha},\theta_{AOA\_RG,n,m}^{\beta}\right)}}$$
$$\xi_{n,m}\emptyset_{n,m}\exp\left(jkd_{BS}^{1}\sin\left(\theta_{AOD\_RG,n,m}^{\alpha}\right)\right)\exp\left(jkd_{BS}^{2}\sin\left(\theta_{AOD\_RG,n,m}^{\beta}\right)\right)$$
$$\exp\left(jkd_{MS}^{1}\sin\left(\theta_{AOA\_RG,n,m}^{\alpha}\right)\right)\exp\left(jkd_{MS}^{2}\sin\left(\theta_{AOA\_RG,n,m}^{\beta}\right)\right)$$
$$\exp(jK[v_{BS}\cos\left(\theta_{AOD\_RG,n,m}^{\alpha}-\gamma_{BS}^{\alpha}\right)\cos\left(\theta_{AOD\_RG,n,m}^{\beta}-\gamma_{BS}^{\beta}\right)+$$
$$v_{MS}\cos\left(\theta_{AOA\_RG,n,m}^{\alpha}-\gamma_{MS}^{\alpha}\right)\cos\left(\theta_{AOA\_RG,n,m}^{\beta}-\gamma_{MS}^{\beta}\right)]t) \quad (16)$$

where $\xi_{n,m}$is the amplitude of macro reflectors and $\emptyset_{n,m}$ denotes the phase of the macro reflectors.

Since the location of local objects in the model is randomly allocated among the transmitter and the receiver, the time of signal propagation is calculated based on the location of the base station, the mobile station, and objects with random coordinates.

**Simulation results**

For each pair of transmitting and receiving antennas, the frequency of the carrier was chosen of 2.5 GHz and bandwidth of 20 MHz which will provide moderate signal attenuation for the selected wireless range. It was assumed that the base station is stationary and occupies a fixed position, while the mobile moves at a certain constant speed. The initial data for modeling are presented in **Table 1**.

**Table1** Channel simulation parameters.

| Parameter | Name | Value | Unit |
|---|---|---|---|
| f | Signal bandwidth | 2.5 | GHz |
| $f_n$ | Carrier frequency | 20 | kHz |
| $h_{BS}$ | Base station height | 50 | m |
| $h_{MS}$ | Mobile station height | 5 | m |
| $R$ | Distance between BS and MS | 4.5 | Km |
| M | Number of subpaths | 20 | |
| $\boldsymbol{N_{TX}}$ | Number of antennas at the TX | 2 | |
| $N_{RX}$ | Number of antennas at the RX | 2 | |
| t | temperature | 16 | C |
| N | Number of paths | 7 | |
| $G_{BS}$ | Gain of BS antennas | 1 | |
| $G_{MS}$ | Gain of MS antennas | 1 | |
| $V_{BS}$ | Velocity of BS | 0 | km/s |
| $V_{MS}$ | Velocity of MS | 30 | Km/s |
| LOS | Line of sight | yes | |
| c | speed of sound | $3 \times 10^8$ | m/s |
| $d_{BS}$ | Distance between the elements of the BS antennas | 0 | m |
| $d_{MS}$ | Distance between the elements of the MS antennas | 0 | m |
| $\sigma_{AoD}$ | The spread of subpaths in AoD | 5° | degree |
| $\sigma_{AoA}$ | The spread of subpaths in AoA | 35° | degree |

The main probabilistic feature of the system includes the probability of a bit error, which is the number of bit errors divided by the total number of bits received in a transmission for a given SNR.

$$BER = \frac{N_{error\ bits}}{N_{total\ bits}} \quad (17)$$

In the simulation, it is assumed that the channel, both pilot and information, is stationary for the duration of one frame of the OFDM symbol (for the next frame, the calculations are repeated). The parameters of the channel would be similar to those used in channel modeling (**Table 1**).

The parameters of the OFDM signal will correspond to the values presented in **Table 2**, in which the number of subcarriers equal to 1,024 is selected with a signal bandwidth of 2.5 GHz. The resulting duration of the entire frame of OFDM symbols will be 0.41 μs, and the cyclic prefix duration will be chosen equal to 1/4 of the signal duration, which will allow avoiding inter symbol interference, according to the obtained maximum signal delay in channel modeling.

**Table 2** Selected OFDM signal parameters.

| Parameter | Name | Value | Unit |
|---|---|---|---|
| N | Total number of subcarriers | 1,024 | |
| $t_g$ | Guard interval duration | ¼ | μs |
| $f_c$ | Carrier frequency | 100 | kHz |
| BW | Signal bandwidth | 2.5 | GHz |
| $t_s$ | OFDM symbol duration | 0.41 | μs |
| n | Number of pilot signals | 150 | |

The number of elements for the adaptation block is 4, the number of elements of the AR should be greater than the number of paths. The distance between the elements of the transmitter is 0.5ʎ, it is chosen as small as possible in order to ensure a high spatial correlation of the signals necessary for adaptation.

At first, we will simulate all nodes of the SISO-OFDM system. In the modeling process, we will consider how the equivalent directional characteristic changes after weight processing in the adaptation

block of **Figure 4** It should be noted that as a result we get the expected result: The maximum directional characteristics directed to the path with maximum power, taking into account the selected simulation parameters, this path is a straight line that has the least attenuation and minimum propagation delay between the transmitter and receiver. According to the simulation results, the direct path has a true value of the angle of arrival equal to 26.5° relative to the perpendicular to the opening of the AR. Moreover, in the direction of arrival of the remaining paths, zeros of the directional characteristic are formed. As a result, the system chose it as the optimal from the point of view of the criterion of maximum average signal power. Consider how adaptive processing influenced the demodulation of information subcarriers of an OFDM signal. To do this, we construct the signal constellation of the demodulated signal in the receiver with and without an adaptation block as shown in **Figure 5**.

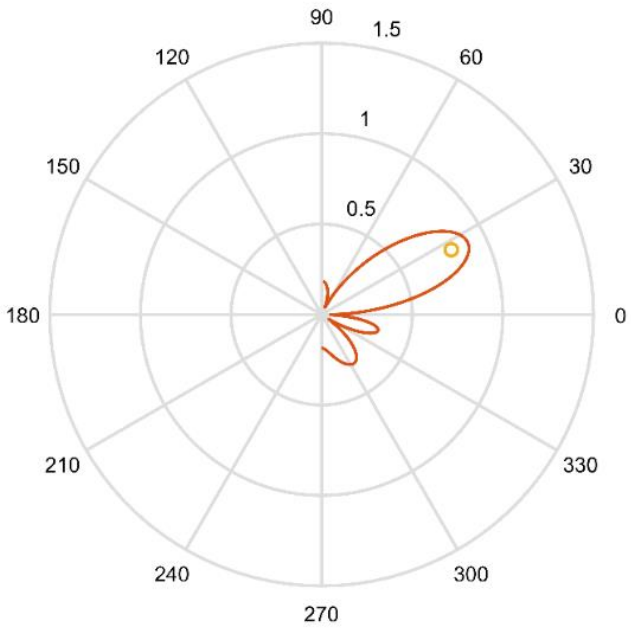


**Figure 4** Adapted MD after weighing at SNR = 10 dB.

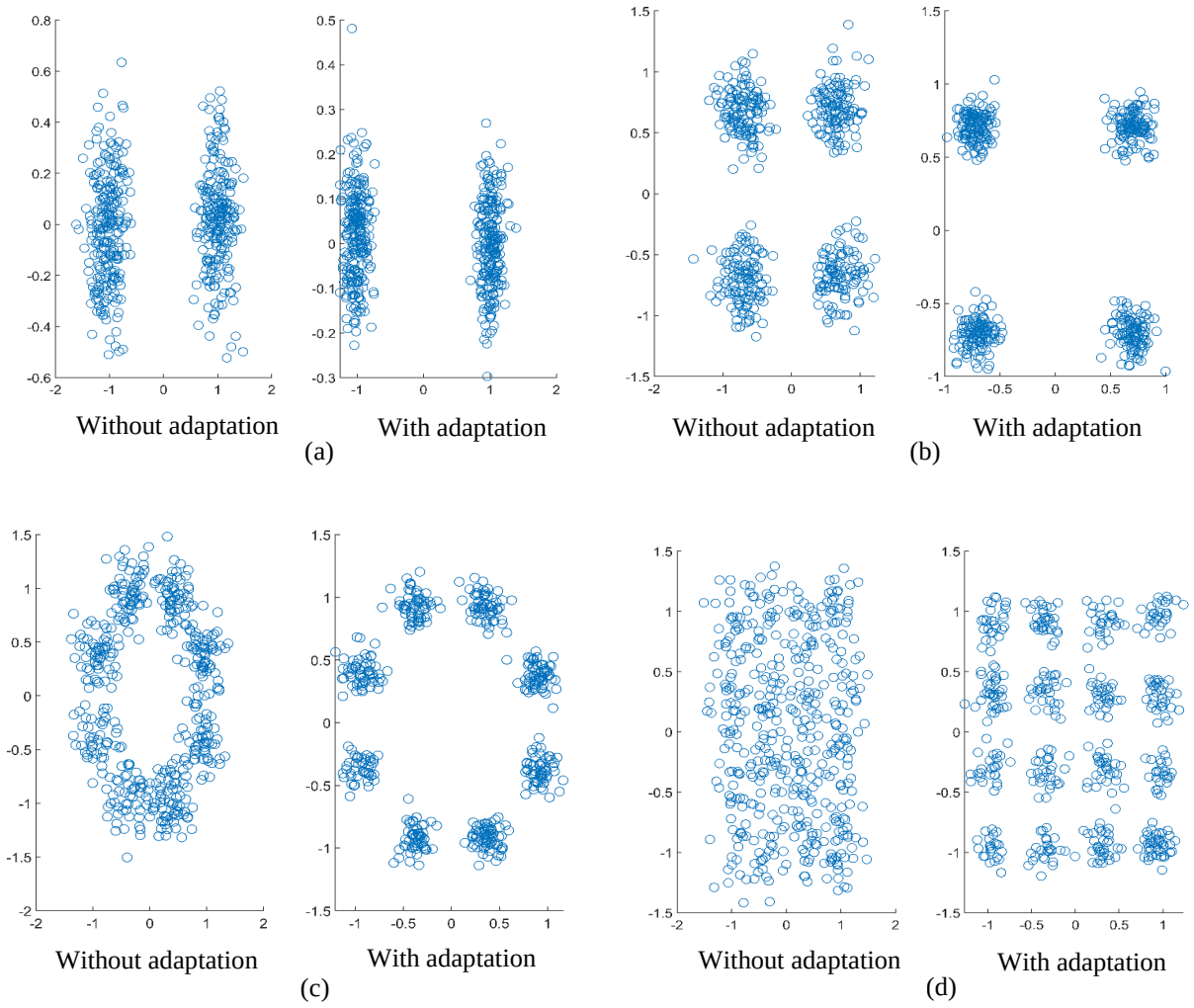


**Figure 5** Signals constellation after demodulation at 10 dB SNR for different type of modulations: (a) BPSK, (b) QPSK, (c) 8-PAM, and (d) 16-QAM.

As shown in this figure, the spread of signal values at the signal constellation is larger in the receiver without the use of an adaptive algorithm. This leads to an increase in the probability of bit error, while for a receiver with adaptive processing, the probability of error approaches 0. To estimate how the bit error probability changes, it is necessary to plot its relationship to the signal-to-noise ratio as shown in **Figures 6** to **9**. As shown in these figures, it can be observed that the signal spread changes according to the changes of the type of modulation, in other words, the signal spread changes according to the changes of order form of modulation and as a results, the bits of information per symbol are changed also. For example, in BPSK modulation, the spread of signal was large due to lower order form of modulation and therefore the error rate becomes very low. For 16-QAM, the error rate will be higher than BER for BPSK due to the higher form of modulation and as a result of this, the spread of signal was small.

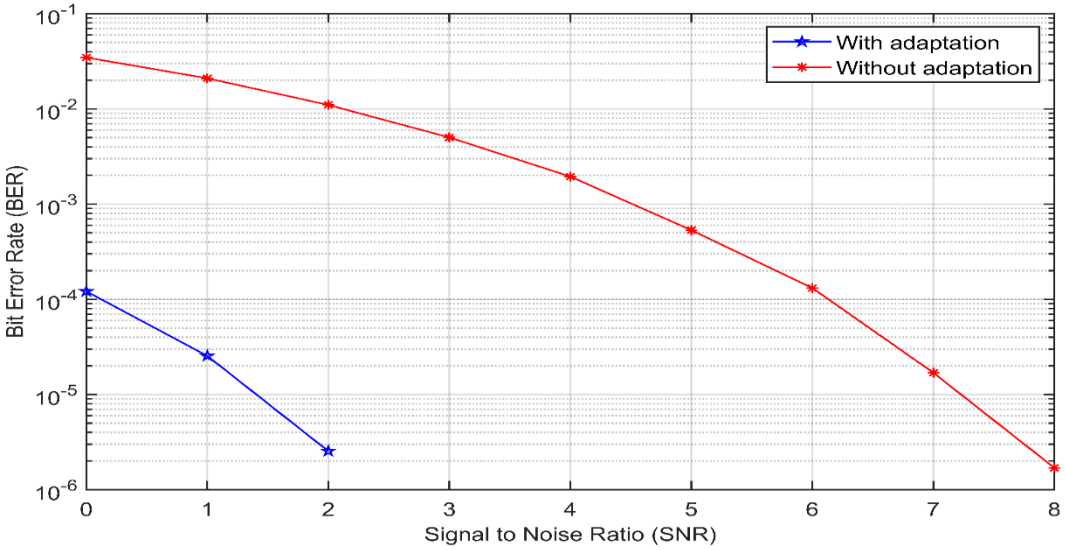


**Figure 6** Bit error probability for adaptive AR algorithm for BPSK modulation.

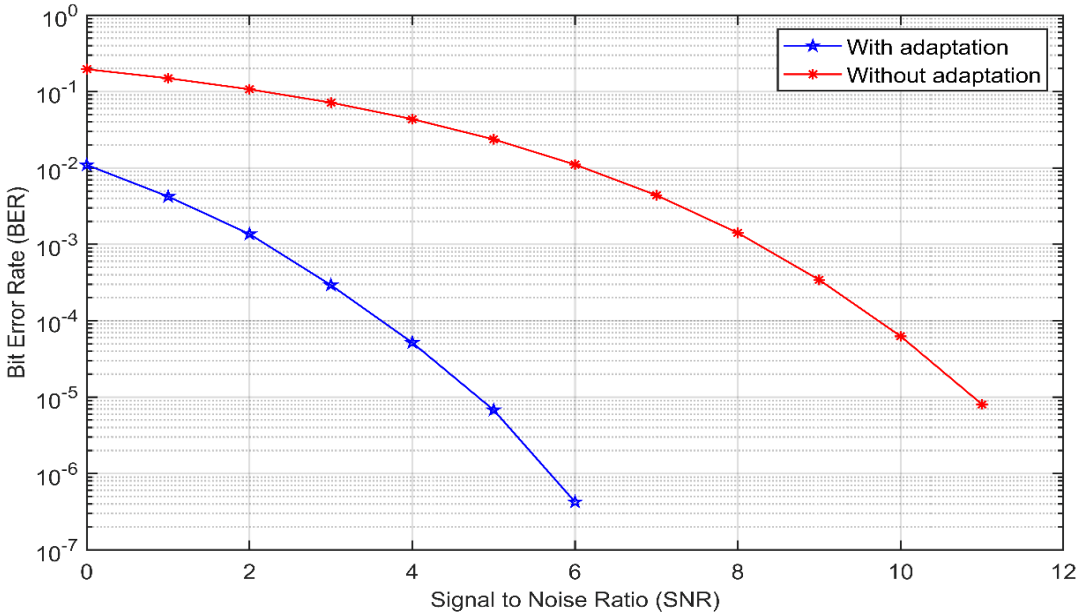


**Figure 7** Bit error probability for adaptive AR algorithm for QPSK modulation.

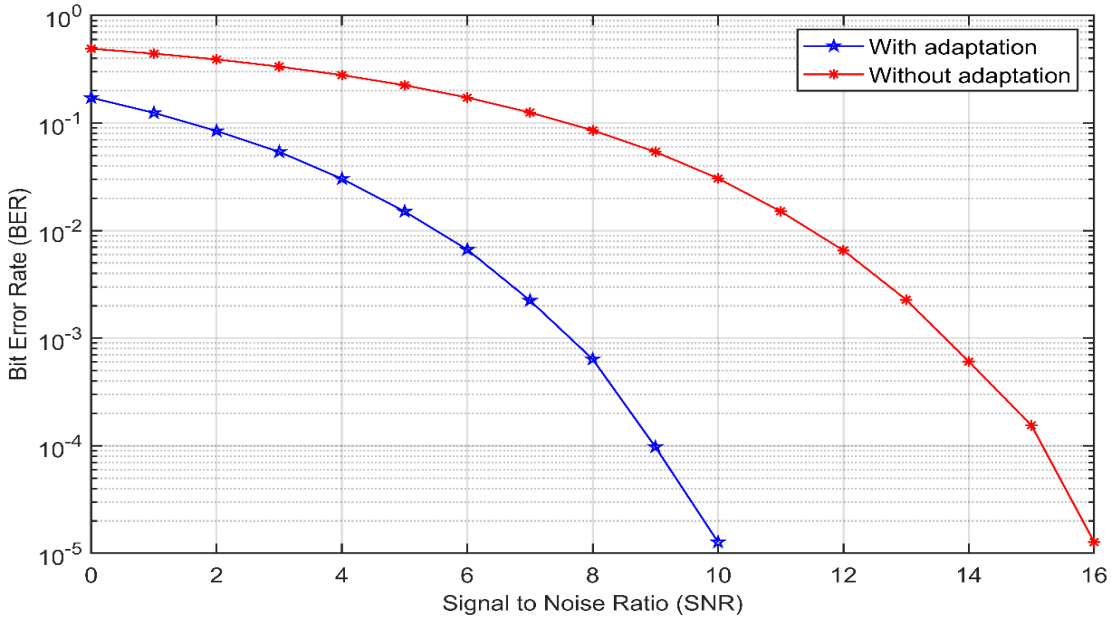


**Figure 8** Bit error probability for adaptive AR algorithm for 8-PSK modulation.

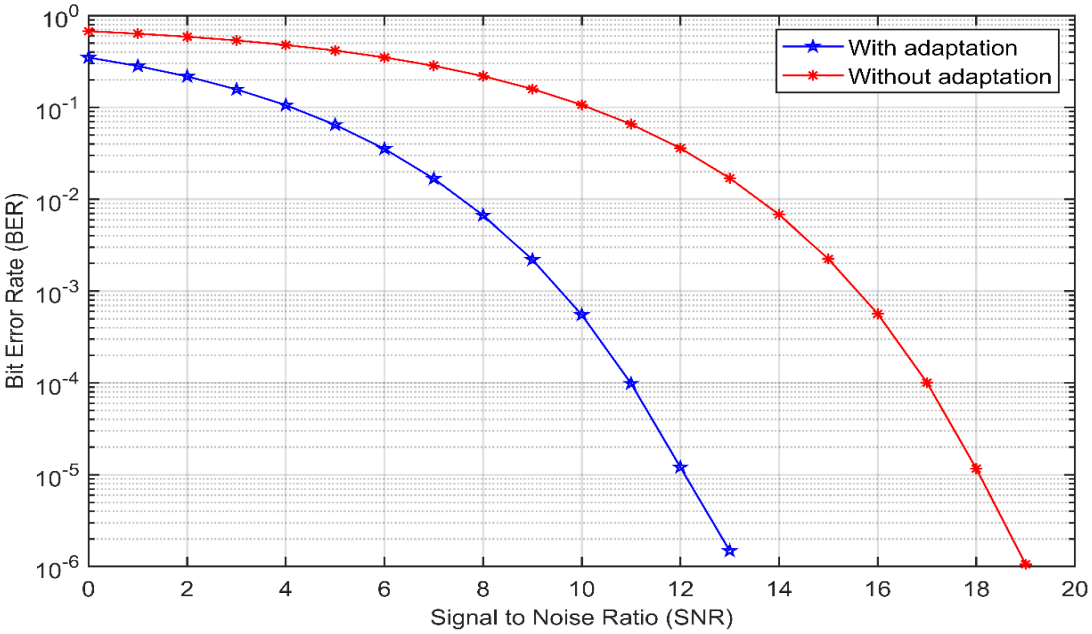


**Figure 9** Bit error probability for adaptive AR algorithm for 16-QAM modulation.

The figures above show that the use of adaptation algorithm reduces the probability of a bit error in the transmitted message. Moreover, the probability of error already at 0 dB differs by more than 2 orders of magnitude. As a result, we can conclude that the use of adaptive algorithms has a positive effect on noise immunity when processing signals in a receiving device under conditions of multi-path signal propagation.

It can be seen also from the figures that the BER changes according to the changes of order form of modulation.

At the MIMO-OFDM system, the experimental conditions will be similar to the previous ones: Channel parameters - **Table 1**, OFDM signal parameters - **Table 2**, the parameters of the antenna system. The parameters are set for MIMO 2×2, the number of elements for each adaptation block is 4, the number of elements of the AR should be greater than the number of paths. The distance between the elements of the AR transmitter. The distance between the elements of the transmitter, it is necessary to choose as little as possible in order to ensure high spatial correlation of the signals necessary for adaptation.

In this experiment, we obtain 2 spatial streams that are recorded by 2 receiving antennas, which are blocks of AR elements, and, therefore, each such block forms its own independent directional characteristic. The radiation patterns at a signal-to-noise ratio of 7 dB for 2 receiving units are shown in **Figure 10**.

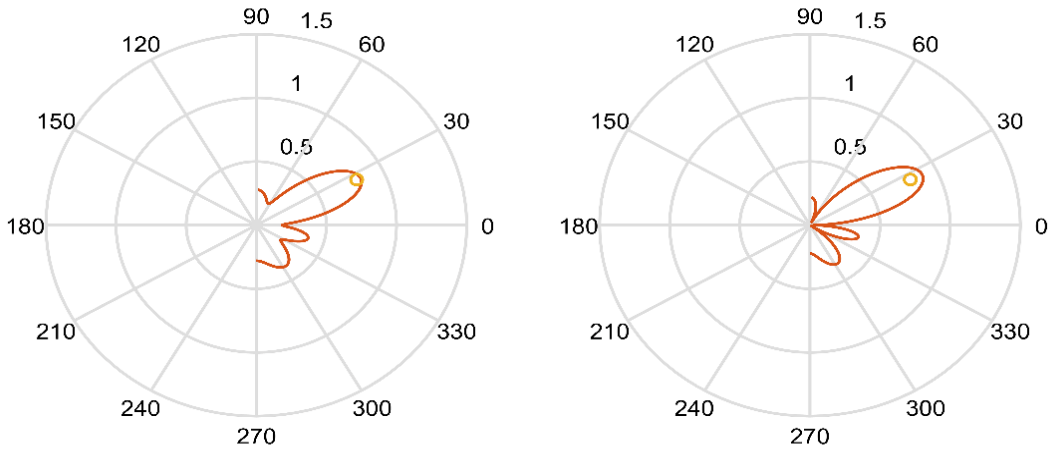


**Figure 10** Adapted radiation pattern for MIMO-OFDM system.

It can be seen from the above figure that, similarly to the SISO system, the adaptive algorithm generated a directional characteristic for each antenna in the direction of the direct path that has the highest power. It should be noted that, in the general case, the type of radiation pattern for the 2 antennas is different, however both have a characteristic maximum in the direction of the direct path. As for the SISO system, the result of adaptive processing can be seen if we consider the signal constellation in the receiver after demodulation of the OFDM signal as shown in **Figure 11**.

Unlike the SISO system in MIMO, each antenna array unit forms a directional characteristic in the direction of signal arrival along the path with maximum power. Therefore, in the general case, the type of directional characteristic for the antenna units may differ, as shown in **Figure 10**. As a result, similarly to the SISO system in the MIMO receiver with adaptive processing, the probability of bit error decreases and this can be clearly noted if we consider how this probability depends on the signal-to-noise ratio as shown in **Figures 12** to **15**.

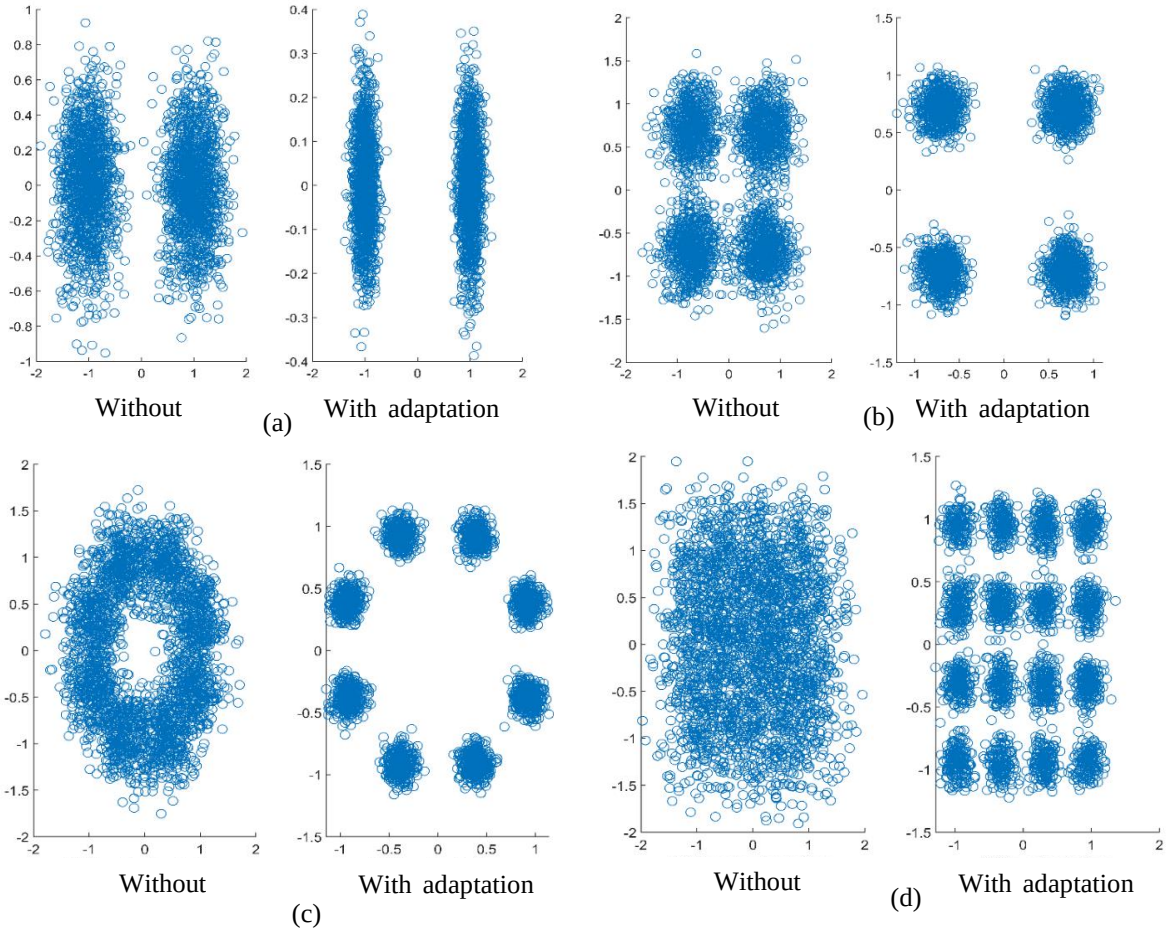


**Figure 11** Signals constellation of demodulated signal at MIMO-OFDM receiver for different types of modulation, (a) BPSK, (b) QPSK, (c) 8-PAM, and (d) 16-QAM.

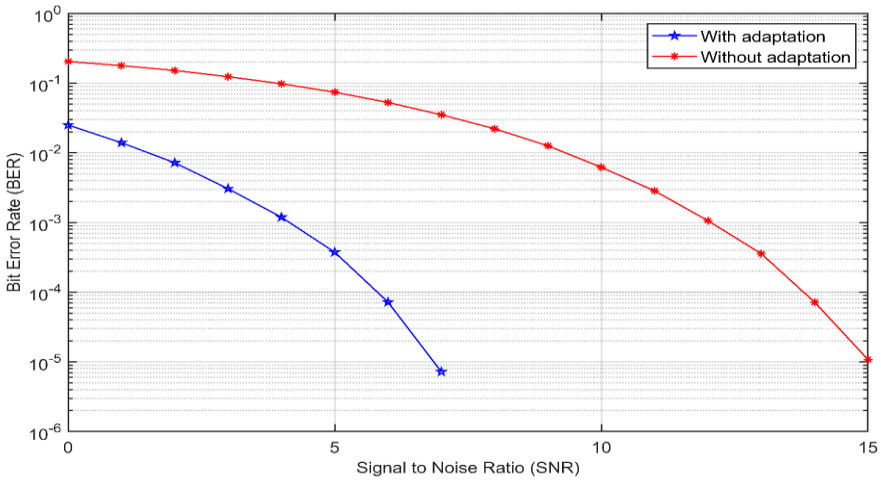


**Figure 12** Bit error probability for MIMO-OFDM system with and without adaptation for BPSK modulation.

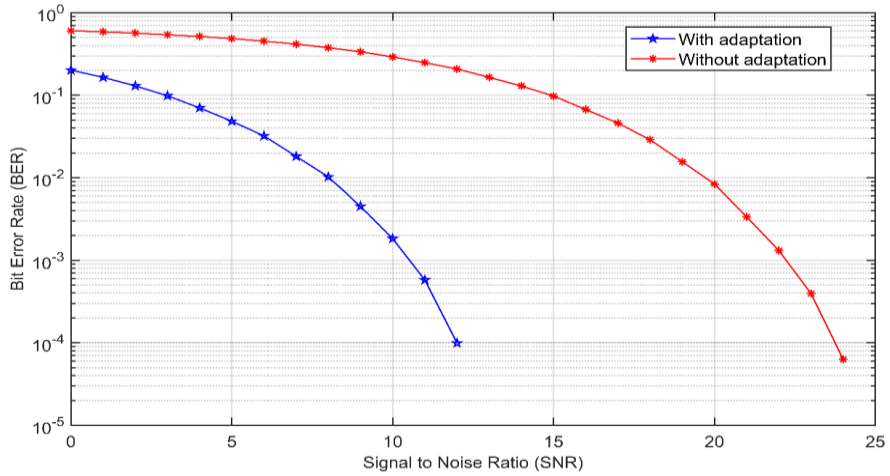


**Figure 13** Bit error probability for MIMO-OFDM system with and without adaptation for QPSK modulation.

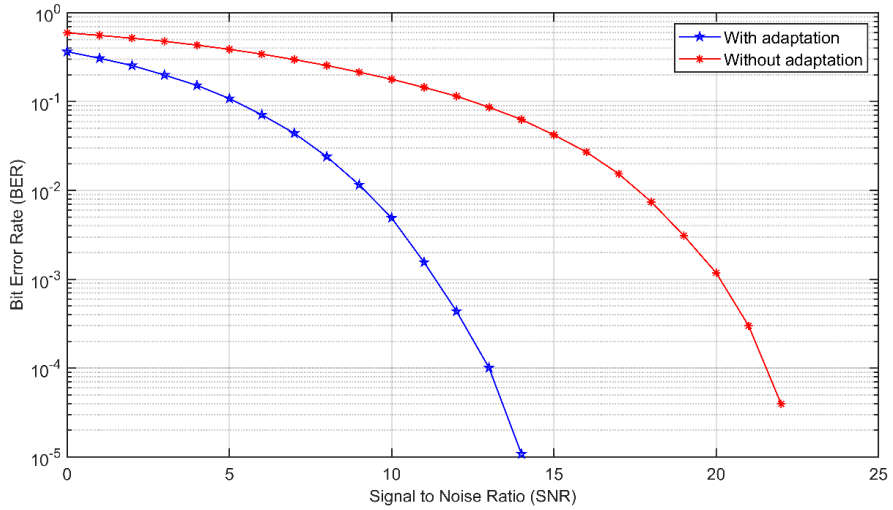


**Figure 14** Bit error probability for MIMO-OFDM system with and without adaptation for 8-PSK modulation.

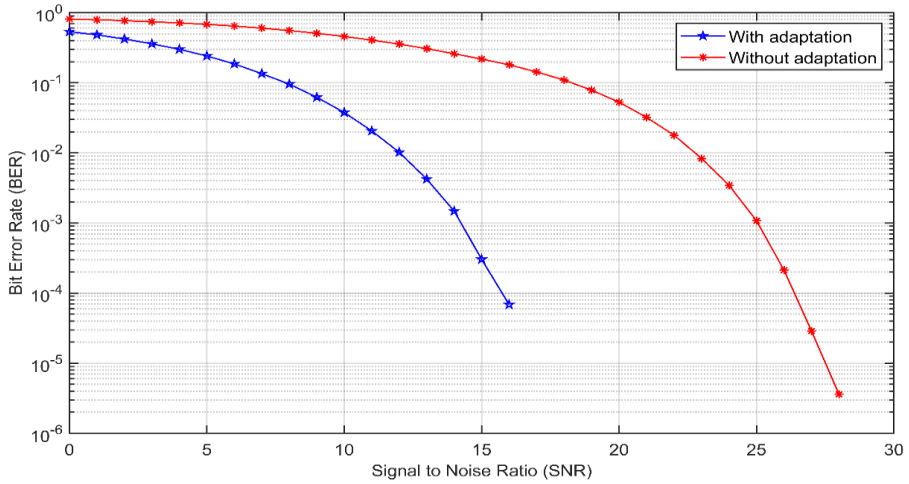


**Figure 15** Bit error probability for MIMO-OFDM system with and without adaptation for 16-QAM modulation.

**Figures 12** to **15** above also show that the probability of BER in the transmitted message is reduced when using adaptation algorithm. As a result, it can be concluded that a positive effect on noise immunity in processing signal at the receiving device when using adaptive algorithm under conditions of multi-path signal propagation. It can be seen also that in MIMO technique when the order form of modulation is changed, the BER changed also.

**Figures 6** to **9** for SISO-OFDM results and **Figures 12** to **15** for MIMO-OFDM results show that the adaptive spatial filtering algorithm allows you to effectively deal with multi-path propagation of signals in a WiMAX channel, both in the presence of a direct path and also in its absence. In addition, adaptation has a positive effect on channel capacity.

## Conclusions

A general algorithm for modeling a 3D WiMAX wireless channel communication system was developed. An algorithm for the adaptive signal processing unit for the amplitude and phase system has also been developed. To compare the efficiency of using adaptive algorithms, the bitstream transmission through all nodes of the 3D WiMAX communication system was simulated taking into account the influence of channel characteristics with and without an adaptation block. As a result, bit error probability characteristics were obtained for SISO and MIMO systems with various adaptation block configurations. For MIMO systems, the dependence of throughput on the number of spatial streams on the signal-to-noise ratio was also constructed using adaptive algorithms and without. The effectiveness of the adaptation algorithms was clearly shown on the signal constellations and antenna patterns after the adaptation unit.

From the results it can be concluded that the use of the adaptation algorithm reduces the probability of error in the transmitted message. Also, it can be concluded that the use of adaptive algorithms has a positive effect on noise immunity when processing signals in a receiving device under conditions of multi-path signal propagation.

## References

[1] R Fantacci, D Marabissi, D Tarchi and I Habib. Adaptive modulation and coding techniques for OFDMA systems. *IEEE Trans. Wirel. Commun*. 2009; **8**, 4876-83.

[2] D Johnston and J Walker. Overview of IEEE 802.16 security. *IEEE Secur. Priv.* 2004; **2**, 40-8.

[3] C Eklund, RB Marks, KL Stanwood and S Wang. IEEE standard 802.16: A technical overview of the WirelessMAN/sup TM/air interface for broadband wireless access. *IEEE Commun. Mag.* 2002; **40**, 98-107.

[4] MA Hasan. 2007, Performance evaluation of WiMAX/IEEE 802.16 OFDM physical layer. Master thesis. Helsinki University of Technology, Espoo, Finland.

[5] S Chen and C Zhu. ICI and ISI analysis and mitigation for OFDM systems with insufficient cyclic prefix in time-varying channels. *IEEE Trans. Consum. Electron.* 2004; **50**, 78-83.

[6] A Barbieri, G Colavolpe, T Foggi, E Forestieri and G Prati. OFDM versus single-carrier transmission for 100 Gbps optical communication. *J. Light. Technol.* 2010; **28**, 2537-51.

[7] BS Reddy, L Boppana, A Srivastava and RK Kodali. Modulation switching in OFDM for WiMAX through Rayleigh fading channel using GNU radio. *In:* Proceedings of the International Conference on Advanced Electronic Systems, Pilani, India. 2013, p. 331-3.

[8] SE Elayoubi and B Fourestié. Performance evaluation of admission control and adaptive modulation in OFDMA WiMax systems. *IEEE ACM Trans. Netw.* 2008; **16**, 1200-11.

[9] J Faezah and K Sabira. Adaptive modulation for OFDM systems. *Int. J. Commun. Netw. Inf. Secur.* 2009; **1**, 1.

[10] S Colieri, M Ergen, A Puri and A Bahai. A study of channel estimation in OFDM systems. *In:* Proceedings of the 56th Vehicular Technology Conference, Vancouver, BC, Canada. 2002, p. 894-8.

[11] VP Fedosov, AV Lomakina, AA Legin and VV Voronin. Modeling of systems wireless data transmission based on antenna arrays in underwater acoustic channels. *In:* Proceedings of the SPIE Commercial + Scientific Sensing and Imaging, Baltimore, Maryland, USA. 2016, p. 98720G.

[12] J Thota, R Almesaeed, A Doufexi, S Armour and AR Nix. Infrastructure to vehicle throughput performance in LTE-A using 2D and 3D 3GPP/ITU channel models. *In*: Proceedings of the IEEE 81st Vehicular Technology Conference (VTC Spring), Glasgow, UK, 2015, p. 1-5.

[13] R Almesaeed, AS Ameen, A Doufexi, N Dahnoun and AR Nix. A comparison study of 2D and 3D ITU channel model. *In:* Proceedings of the IFIP Wireless Days, Valencia, Spain. 2013, p. 1-7.

[14] V Fedosov, A Legin and A Lomakina. Algorithms based on MIMO-OFDM technology for realization of digital hydroacoustic communication channel. *Izv. SfedU. Eng. Sci.* 2015; **168**, p. 148-58.
[15] V Fedosov, A Legin and A Lomakina. Adaptive algorithm for data transmission in wireless channels based on MIMO-OFDM technique. *In:* Proceedings of the Radiation and Scattering of Electromagnetic Waves, Divnomorskoe, Russia. 2017, p. 218-21.
[16] C Lee, KM Cheung and V Vilnrotter. Fast eigen-based signal combining algorithms for large antenna arrays. *In:* Proceedings of the IEEE Aerospace Conference Proceedings (Cat. No.03TH8652), Big Sky, MT, USA. 2003, p. 1123-9.
[17] M Ratynskii. *Adaptation and superresolution in antenna arrays*. Radio i Svyaz', Moscow, 2003.
[18] YH Nam, Y Li and JC Zhang. 3D channel models for elevation beamforming and FD-MIMO in LTE-A and 5G. *In:* Proceedings of the 48th Asilomar Conference on Signals, Systems and Computers, Pacific Grove, CA, USA. 2014, p. 805-9.
[19] YS Cho, J Kim, WY Yang and CG Kang. *MIMO-OFDM wireless communications with MATLAB.* John Wiley & Sons, New Jersey, USA, 2010, p. 544.
[20] VP Fedosov, AV Lomakina, AA Legin and VV Voronin. Three-dimensional model of hydro acoustic channel for research MIMO systems. *In:* Proceedings of the SPIE Defense + Security, Anaheim, California, USA. 2017, p. 101860W.
[21] F Ademaj, M Taranetz and M Rupp. 3GPP 3D MIMO channel model: A holistic implementation guideline for open-source simulation tools. *Eurasip J. Wirel. Commun. Netw.* 2016; **2016**, 1-14.
[22] MW Khan, Y Zhou and G Xu. Modeling of acoustic propagation channel in underwater wireless sensor networks. *In:*Proceedings of the 2nd International Conference on Systems and Informatics, Shanghai, China. 2014, p. 586-90.
[23] AG Zajic. Statistical modeling of MIMO mobile-to-mobile underwater channels. *IEEE Trans. Veh. Technol.* 2011; **60**, 1337-51.
[24] L Zhang, J Liu, K Liu and Y Zhou. On the 3D beamforming and proactive cell shaping with 3GPP 3D channel model. *In:* Proceedings of the IEEE Globecom Workshops, Austin, TX, USA. 2014, p. 688-93.